

Direct Measurement of Interaction Forces between Islands on Freely Suspended Smectic C Films Using Multiple Optical Tweezers

A. Pattanaporkratana¹, C. S. Park², J. E. Maclennan³, and N. A. Clark⁴

Liquid Crystal Materials Research Center, Department of Physics,
University of Colorado, Boulder, CO 80309, USA

¹e-mail: pattanap@Colorado.EDU; ²e-mail: cpark@bly.Colorado.EDU;

³e-mail: jem@Colorado.EDU; ⁴e-mail: clarkn@Colorado.EDU

Smectic liquid crystals can be made to form freely suspended films, two-dimensional systems locally quantized in thickness by an integral number of smectic layers, on which islands, circular regions of greater thickness than the surrounding film area, can be generated. In smectic C films, each such island is accompanied by a topological defect pair, an $s = +1$ topological defect inside and an $s = -1$ defect nearby on the background film. The distortions of the in-plane orientational order of the smectic C director field result in elastic interactions between the islands, with a short-range repulsion and a long-range dipolar attraction governing their stability and leading to their organization in chain-like structures with an equilibrium island separation. We demonstrated previously that such islands can be manipulated using optical tweezers. Using an acousto-optically scanned infrared laser system to generate dynamically controllable, multiple optical traps, we have now directly measured the repulsive and attractive elastic interaction forces between smectic C islands and have compared the results quantitatively with theory. We find that the interactions between islands are much smaller in the racemic smectic C case than in the chiral smectic C*, an effect we attribute to long-range coulombic forces arising from polarization charges.*

I. Introduction

Smectic liquid crystals are known to form stable free-standing films similar to soap films when they are stretched on a solid frame. The structure and mechanical and thermodynamical properties of films have been widely studied since they were discovered by Friedel in 1922[1,2]. Investigations of topological defects and the self-organization of circular inclusions in smectic C (SmC) free-standing films are quite recent [3–8]. Pettey *et al.* [3] derived an expression for the director field associated with islands containing topological defects by minimizing the Frank elastic free energy of a smectic C film in 2D, assuming fixed boundary conditions on a circular disk on the film representing the island, and showed that there is a hyperbolic -1 point defect at a distance $\sqrt{2}R$ from the center where R is the disk radius. Patricio *et al.* [9] calculated the effective interaction energy between two such circular disks immersed in a smectic C film using finite element, adaptive mesh methods to minimize the elastic free energy numerically. Their model shows short-range repulsive and long range attractive interactions between the two disks, with a minimum in the elastic energy at a disk separation $D = 2\sqrt{2}R$. Recently, Cluzeau *et al.* [10] have reported chaining of nematic

inclusions and their accompanying hyperbolic defects on smectic C films. None of these studies, however, have measured the elastic interaction forces between circular inclusions in 2D experimentally.

In our experiments, smectic islands, which are disk-shaped, thicker regions, are generated on freely suspended films by in-plane shear produced by opposed gas jets. The island diameters are in the range $1 < R < 100 \mu\text{m}$ and they are typically up to ten times thicker ($N \sim 20$ layers) than the surrounding liquid crystal film of $N_f \sim 2$ layers. In chiral films, the islands spontaneously form pairs or linear chains. Polarizing optical reflection microscopy was used both to visualize the islands and to map the *c*-director field (the projection of the tilted molecules in the layer plane). The *c*-director anchoring at the island boundary is tangential and a hyperbolic -1 defect is associated with each island. We have shown previously that islands on freely suspended smectic films can be manipulated using optical tweezers [11]. In this report, we describe how an acousto-optically scanned IR laser system is used to generate dynamically controllable, multiple optical traps. Using these optical tweezers with variable trapping force, we can directly measure the elastic forces between smectic C islands and compare the results quantitatively with theory. We find that the measured interaction forces between islands in the chiral smectic C* are much stronger than in racemic smectic C films.

II. Experimental

We have used two liquid crystal materials, the chiral mixture MX8068 (Displaytech, Inc., $X \xrightarrow{-22^\circ\text{C}} \text{SmC}^* \xrightarrow{60.5^\circ\text{C}} \text{SmA}^* \xrightarrow{78^\circ\text{C}} \text{N}^* \xrightarrow{80.5^\circ\text{C}} \text{I}$) and its racemic version, all experiments being performed at room temperature (25°C). The islands were observed using a reflected light microscope with infinity-corrected optics.

For tweezing, we used a CW diode laser (CrystaLaser Nd:YAG 2W) with wavelength $\lambda_0 = 1064 \text{ nm}$ and power $\sim 2 \text{ W}$. The laser intensity was controlled by varying the angle between two Glan-Thomson prism polarizers inserted in the beam path. An acousto-optic deflector (IntraAction Corp. Model DTD-274HD6) was used to generate multiple time-sharing optical traps. The tweezing laser beam was brought in using a beam splitter placed just above the objective lens (see Figure 2.1), ending up normally incident to the film surface and tightly focused by the 40X objective. Images of the islands and the surrounding film were recorded using a digital video camera.

Although smectic islands sometimes form spontaneously while creating fresh films, additional islands can be generated by rapidly flowing air over the film surface. Two opposing gas jets induce shear flow in the film, which tears any excess material on the film or near the meniscus into small pieces. These fragments then become islands, adopting a circular perimeter because of line tension. The air-blowing method rapidly produces a large, polydisperse collection of islands on the film.

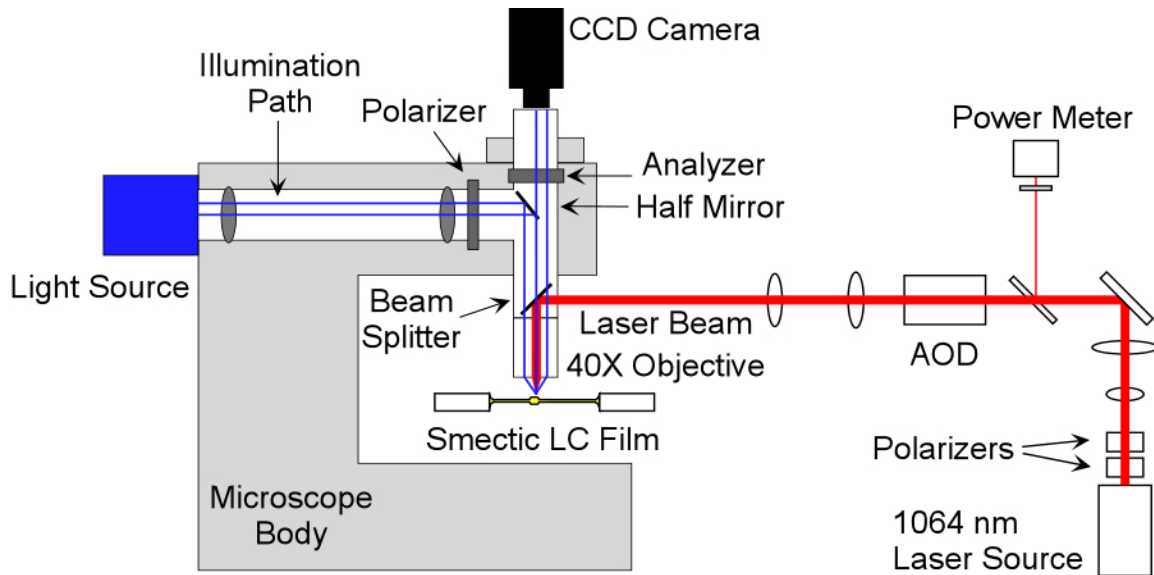


Figure 2.1: Experimental setup for observing and optically trapping islands on smectic films. The films are freely suspended across a 6 mm diameter hole in a microscope cover slip and observed in a polarizing reflection microscope. A computer-controlled acousto-optic deflector (AOD) steers an IR laser to create multiple time-shared optical traps.

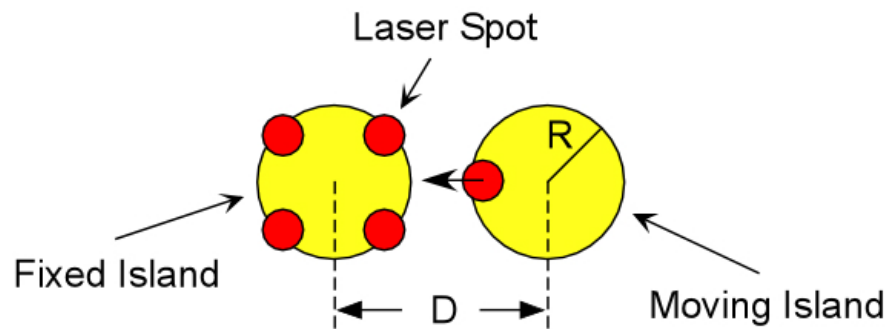


Figure 2.2: Measuring the interaction force between islands using optical tweezers. The island on the left is fixed by four time-sharing optical traps while another trap slowly moves the other island away from its equilibrium position, either further from or closer to the fixed island. At each separation, the laser power is reduced until the island almost escapes the trap, at which time the optical trapping force is equal in magnitude to the elastic restoring force.

We use optical tweezers to pick two islands of approximately the same size and bring them to an isolated place on the film to probe their interaction potential. Figure 2.2 illustrates how laser tweezers are used to measure directly the interaction force between islands on a smectic C film. The island on the left is fixed by four time-sharing optical traps. Another time-sharing trap then slowly moves the island on the right away from its equilibrium position. The maximum displacement of the movable island from its equilibrium position as a function of laser power gives a direct measure of the interaction

potential. If the trapping force is smaller than the repulsive (or attractive) elastic restoring force, then the island escapes from the trap.

The laser power was measured using a power meter, monitoring a 4% portion of the beam reflected from a beam splitter and then filtered (see Figure 2.1). The laser power was calibrated against hydrodynamic drag force to determine the optical force on the movable island, as outlined below.

2.1 Optical Trapping Force Calibration

The optical trapping force on an island as a function of laser power was measured independently by determining the terminal velocity of the island when dragged along the film by the laser. At fixed laser intensity, we begin to drag the island by moving the beam, slowly increasing the scan rate, until above a certain speed, the trapping and drag forces balance and the island escapes from the trap. The hydrodynamic drag force is given by

$$F_d = \frac{4\pi\eta d v}{\ln(R_f / R) - 0.5}$$

where η is the viscosity and d the thickness of the film, v is the velocity of the island, R_f the radius of the film holder, and R the radius of the island [12]. This expression assumes that an island may be modeled as a rigid right cylinder extending through the thickness of the film, with its rotational symmetry axis perpendicular to the film plane. We neglect any interactions with the surrounding air and ignore the anisotropy of the LC fluid. We have taken η as 0.4 poise = 0.04 kg.s/m, the bulk rotational viscosity for rotation on the tilt cone of MX8060. The film thickness was determined using optical reflectivity measurements, the reflectivity for thin films being proportional to thickness squared [16]. All films in our experiments were $N_f = 2$ layers thick.

The optical trapping force, calculated by considering the dielectric energy gradient at the edge of an island, is linearly proportional to laser power [11]. The maximum drag force as a function of incident laser power, shown in Figure 2.3, increases linearly with laser power as expected from theory but the optical tweezing forces obtained in this way are less by a factor of 20 than predicted. The trapping force also depends on island thickness. We did not measure the thicknesses of islands in our experiment because the beam spot of the laser we used for reflectivity measurements was bigger than the typical island diameters but we did recalibrate the optical force hydrodynamically for each new pair of islands.

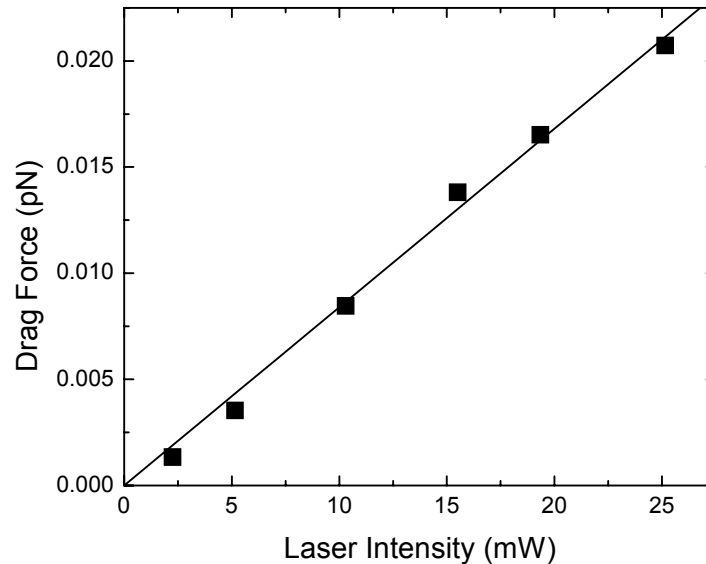


Figure 2.3: Maximum hydrodynamic drag force on an island vs. laser power. The optical tweezing force on the island is assumed to be equal to the maximum achievable drag force.

III. Results and Discussion

In the theoretical simulations by Patricio *et al.* [9], each circular island nucleates a topological defect pair, an $s = +1$ topological defect inside with an $s = -1$ defect nearby on the background film. The equilibrium distance D between the centers of the islands, calculated by minimizing the elastic free energy as a function of the disk separation, was found to scale as $D/R_{ave} \approx 2.82$ where R_{ave} is the average island radius. Over a relatively wide range of island radius, our experimental observations give $D/R_{ave} = 2.94 \pm 0.04$ as shown in Figure 3.1, in fair agreement with the predicted value.

We now discuss in some detail the nature of the interaction between islands on a smectic C film. Distortions of the in-plane orientational order of the smectic C director field result in elastic interactions between the islands, with a short-range repulsion and a long-range attraction leading to an equilibrium island separation and spontaneous organization in chain-like structures.

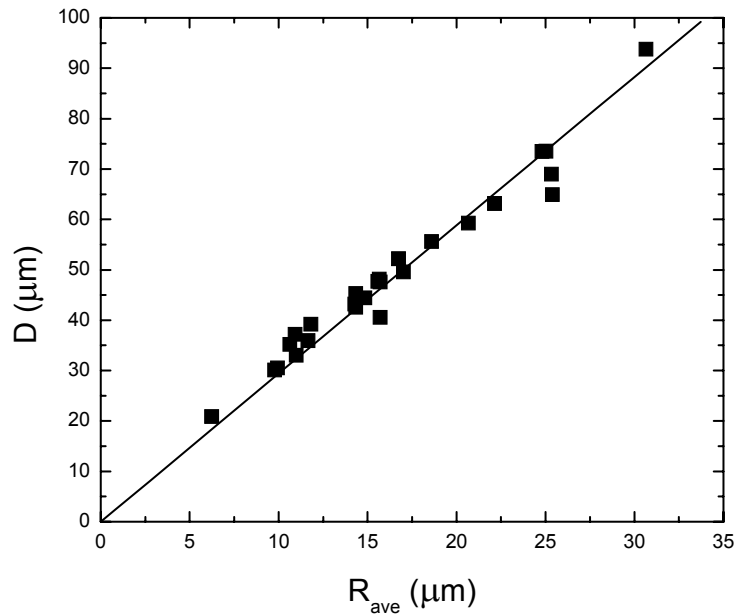


Figure 3.1: Equilibrium distance D between the centers of pairs of smectic C islands in 25% chiral MX8068 films as a function of their average radius R_{ave} . The slope of the fitted line is 2.94.

In order to probe the interaction potential, we have measured the force between islands as a function of their separation using optical tweezers. The results for a 100% chiral MX8068 film are shown in Figure 3.2. The short range repulsive force increases sharply as the islands get closer together and the long range attractive force shows power law decay. This measured force curve is similar to the theoretical force function, plotted as a solid curve in Figure 3.2, computed as the gradient of the interaction energy between inclusions calculated by Patricio *et al.* [9]. We fitted the theoretical curve to the experiment using two fitting parameters, K_{eff} and R_{eff} , where K_{eff} is an effective 2D elastic constant and R_{eff} an effective island radius. Even though the theoretical force curve reflects the experimental trends, the 3D elastic constant $K_{3D} = K_{eff}/d = 56$ pN obtained from fitting, where d is the film thickness, is much greater than the typical value of $K_{3D} \sim 10$ pN [17]. This result is reminiscent of the increase in the effective elasticity for certain modes due to polarization charge observed in several dynamic light scattering experiments on SmC* films and cells [18].

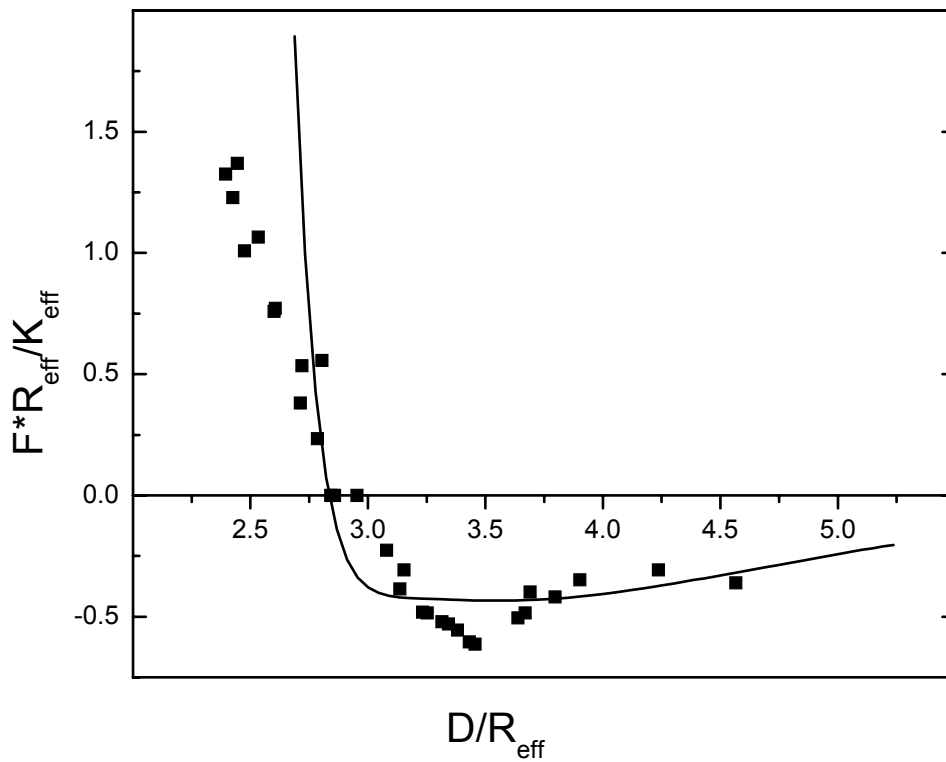


Figure 3.2: Force F between chiral smectic C^* islands on a freely suspended film (100% chiral MX8068) as a function of their separation D , plotted in dimensionless form. The solid line is the best fit derived from the elastic potential energy obtained by Patricio *et al.* [9]. These data are for a pair of islands with average radius $R_{ave} = 12.5 \mu\text{m}$, on a 2-layer film. The islands were in the range 5-30 layers thick. The fit corresponds to $K_{3D} = 56 \text{ pN}$ and $R_{eff} = 1.08 \cdot R_{ave}$.

3.1 Polarization Charge Effects

We have studied films of SmC mixtures with different polarization, from racemic to pure chiral mixtures, in order to explore the influence of polarization fields on the island interaction potential.

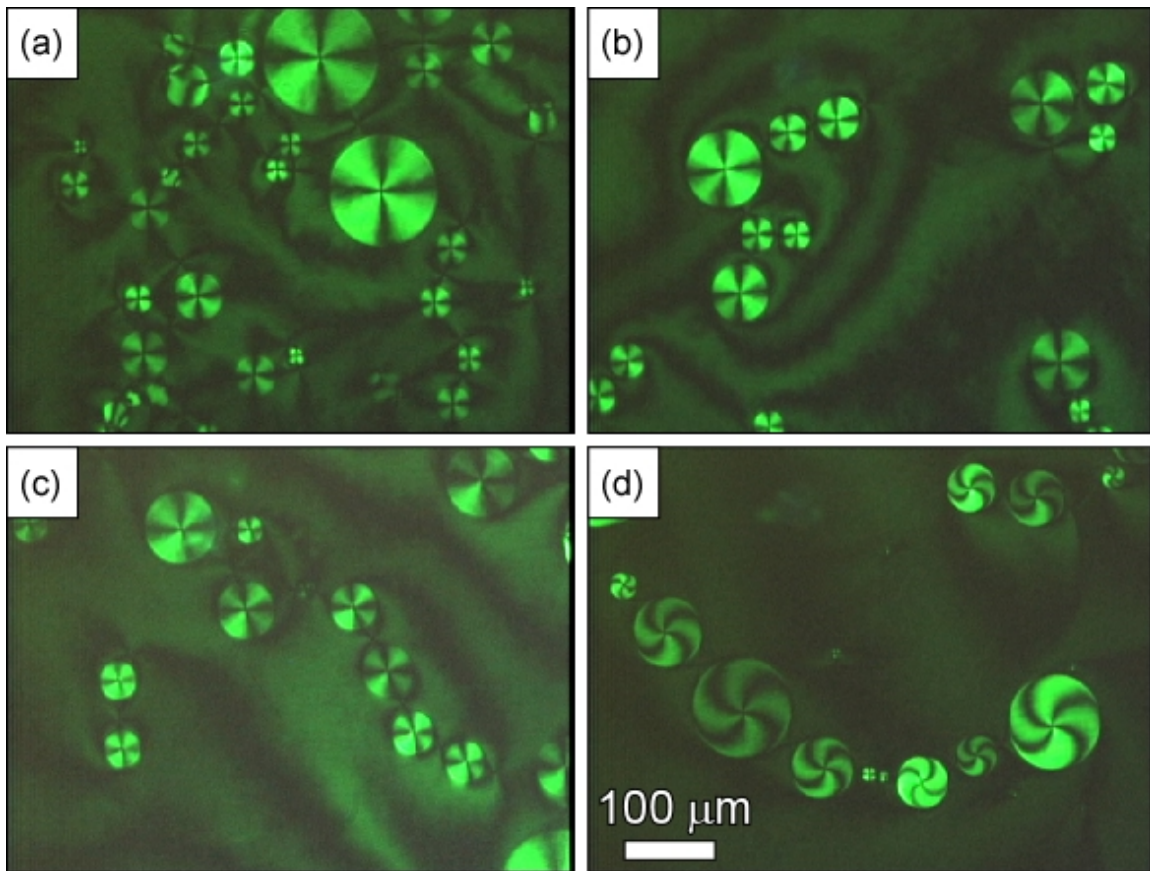


Figure 3.3: Microscope images, obtained in reflection between crossed polarizers, of smectic C islands in MX8068 films, showing typical brush texture and chaining behavior as a function of chiral concentration: (a) racemate; (b) 10% chiral mixture; (c) 25% chiral mixture; (d) 100% chiral enantiomer. With increasing enantiomeric excess we see a greater tendency for island chaining and a transformation from radial to spiral brushes. The length scale in all images is the same.

Figure 3.3 shows microscope images of smectic C islands for various MX8068 mixtures. In the racemate, shown in Figure 3.3(a), there is no apparent chaining and the islands are randomly distributed on the film. The measured inter-island forces are vanishingly weak. With increasing enantiomeric excess (Figures 3.3(b)-(d)), we see a greater tendency for island chaining and eventually a transformation from radial to spiral brushes. The experimental force curve for the case of 25% chiral MX8068 is shown in Figure 3.4. In this case, the elastic constant obtained from fitting is $K_{3D} = 11$ pN which is much smaller than the value $K_{3D} = 56$ pN found in the 100% chiral mixture (Figure 3.2) and much closer to the expected value. The interactions of islands in the film with lower polarization thus seem to be predominantly elastic in origin.

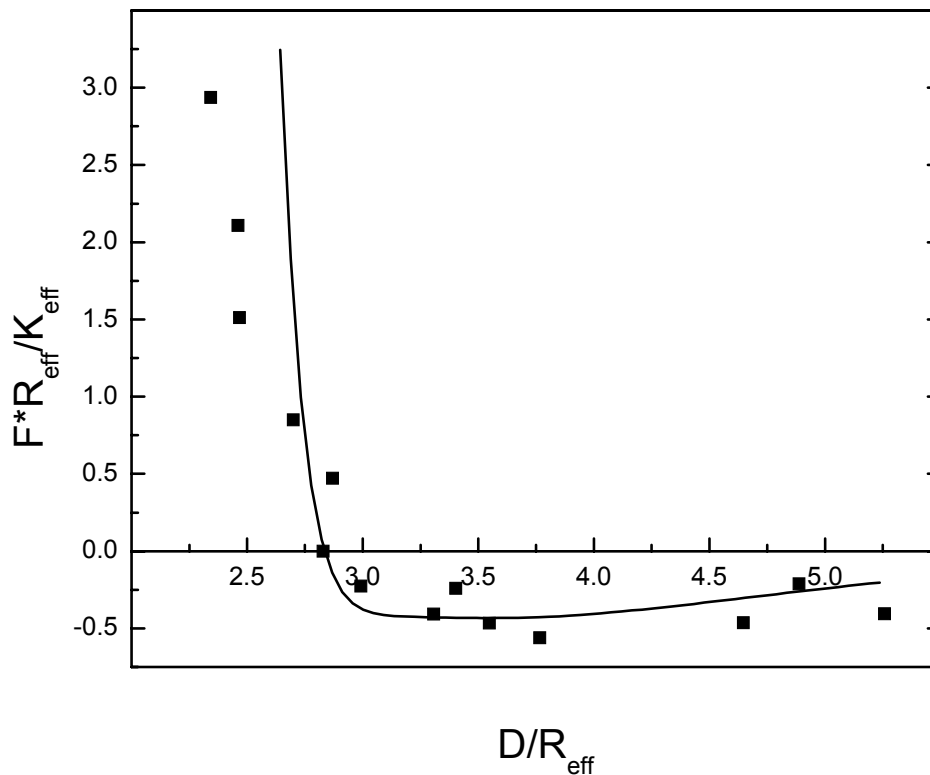


Figure 3.4: Experimentally measured force between a pair of chiral smectic C* islands on a freely suspended smectic film (25% chiral MX8068 mixture). The solid line is the best fit to the data based on the elastic interaction energy calculation results of [9]. In this experiment, $R_{\text{ave}} = 13.3 \mu\text{m}$ and the fit corresponds to $K_{3D} = 11 \text{ pN}$, with $R_{\text{eff}} = 1.18 \cdot R_{\text{ave}}$. The islands were in the range 5-30 layers thick and the background film had $N_f = 2$.

The textures of the islands themselves are also affected by the polarization. In all of our experiments, the c-director (the projection of molecular long axis on layer plane) at the island boundary was found to be tangential (see Figure 3.5). In low polarization mixtures, the c-director around the +1 topological defect at the center of each island is also tangential. In the 100% chiral material, where the polarization is higher ($P = 21 \text{ nC/cm}^2$), while the alignment of the c-director at the island edge is tangential, the c-director rotates as it goes toward the island interior, becoming radial at the core of the defect, reducing polarization splay. This texture is manifest as spiral brushes when viewed between crossed polarizers [14].

It seems clear, therefore, that the spontaneous polarization must be considered in order to account in detail for the interactions of chiral islands. In addition to the distributed polarization charge associated with distortions of the director field around the topological defects, the radial \mathbf{P} at the island boundary leads to an additional accumulation of polarization charge there because of the discontinuity in film thickness. The resulting coulombic interactions are non-local, although the main contributions come

from regions in the orientation field where $\nabla \cdot \mathbf{P}$ is highest, near the ± 1 defects as sketched in Figure 3.5.

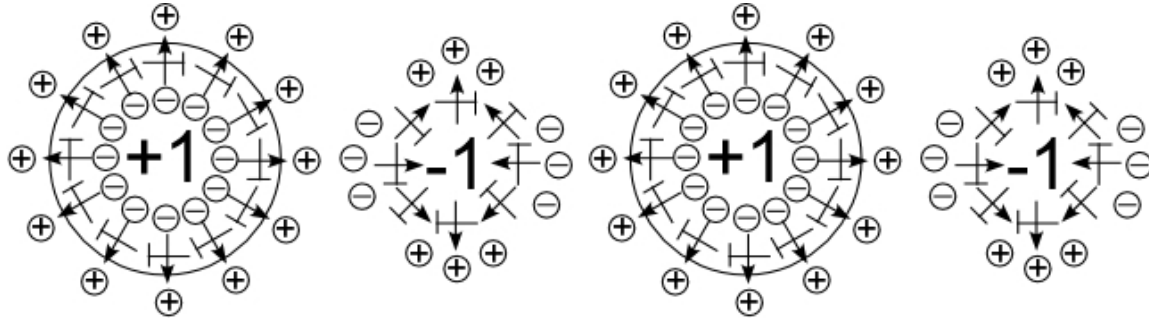


Figure 3.5: Observed c-director/polarization orientation field on SmC films. The islands have tangential c-director \perp (radial polarization \rightarrow) orientation at their boundaries, creating $s = +1$ topological defects inside. Each island has an $s = -1$ companion defect nearby on the background film. \oplus and \ominus represent the polarization charge, present wherever the polarization has non-zero divergence.

Since the attractive elastic force decays as D^{-3} [3], when the separation D between islands is large the elastic contribution to the interaction energy becomes small. The coulombic energy associated with all of the polarization charges in the film, which is significant even for the case of large island separation, is given in by

$$U_{Coulomb} = \frac{P^2}{2\varepsilon} \int d^3r \int d^3r' \frac{\nabla \cdot \hat{p}(r) \nabla \cdot \hat{p}(r')}{|r - r'|}$$

where \hat{p} is a unit vector along the polarization vector \mathbf{P} , and ε is the average of the permittivity coefficients [19]. If we can consider the polarization charge to be clustered principally about the topological defects, with details of the c-director/polarization orientation field to first order independent of the island separation, then the magnitude of the coulombic energy should be quadratic in P . We measured the maximum attractive force between islands in films with different chiral composition, artificially separating the islands to $D \sim 3.5R$ using optical tweezers. The results are shown in Figure 3.6. Since P is proportional to the enantiomeric excess [15], the attractive force due to the polarization charge should be roughly proportional to P^2 , at least in high P materials. This effect is qualitatively confirmed by the data.

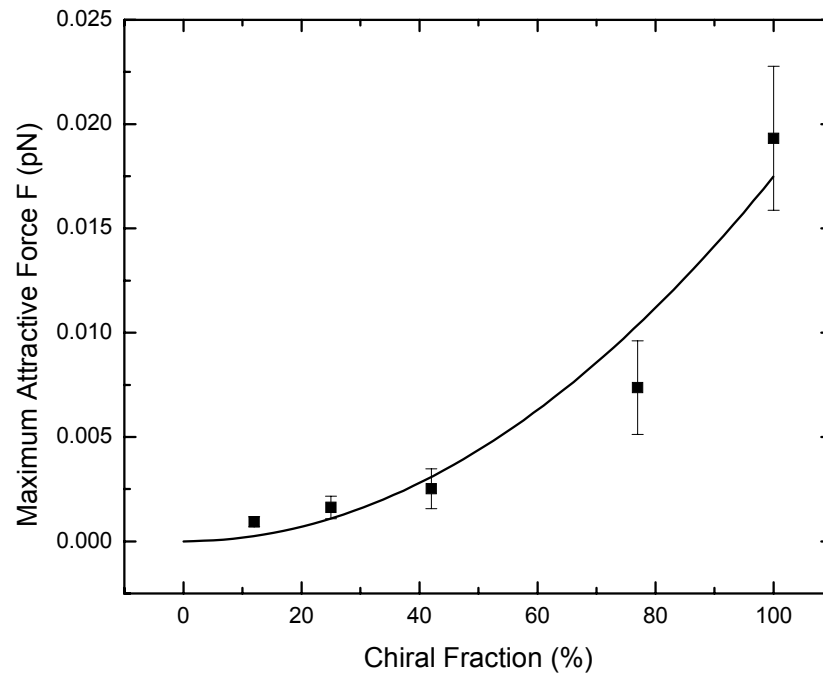


Figure 3.6: Experimentally measured attractive force between islands in MX8068 films with different enantiomeric excess at $D = 3.5R_{ave}$. The solid line is the best quadratic fit to the data. R_{ave} was in the range of 8-17 μm for the ~ 30 island pairs studied in this experiment.

IV. Conclusions

We have directly measured the static interaction force between islands on freely suspended smectic C films using multiple optical tweezers. The interaction potentials can be fitted approximately with theoretically computed two dimensional elastic energy curves, but in chiral films the elastic constant so obtained is significantly greater than the values typically found in other experiments. We suggest that an attractive coulombic force that depends essentially quadratically on the magnitude of the spontaneous polarization needs to be considered in addition to elastic forces in order to explain the interactions between islands in detail.

V. Acknowledgements

This work was supported by NASA Grant NAG-NNC04GA50G and NSF MRSEC Grant No. DMR 0213918. We thank Displaytech, Inc. for kindly providing liquid crystal materials and Instec, Inc. for help with the optical tweezer development.

VI. References

- [1] G. Friedel, *Ann. Phys. (Paris)* **18**, 273 (1992).
- [2] A useful collection of papers on smectic films can be found in P. S. Pershan, *Structure of Liquid Crystal Phases* (World Scientific, Singapore, 1988).
- [3] D. Pettey, T.C. Lubensky, and D. R. Link, *Liq. Cryst.* **28**, 579 (1998).
- [4] P. Cluzeau, V. Dolganov, P. Poulin, G. Joly, and H. T. Nguyen, *Mol. Cryst. Liq. Cryst.* **364**, 381 (2001).
- [5] P. Cluzeau, P. Poulin, G. Joly, and H. T. Nguyen, *Phys. Rev. E* **63**, 031702 (2001).
- [6] P. Cluzeau, V. Bonnand, G. Joly, V. Dolganov, and H. T. Nguyen, *Eur. Phys. J. E* **10**, 231 (2003).
- [7] P. Cluzeau, G. Joly, H. T. Nguyen, and V.K. Dolganov, *JETP Lett.* **75**, 482 (2002).
- [8] P. Cluzeau, M. Ismaili, A. Anakkar, M. Foulon, A. Babeau, and H. T. Nguyen, *Mol. Cryst. Liq. Cryst.* **362**, 185 (2001).
- [9] P. Patricio, M. Tasinkevych, and M.M. Telo da Gama, *Eur. Phys. J. E* **7**, 117 (2002).
- [10] P. Cluzeau, F. Bougrioua, G. Joly, L. Lejcek, and H. T. Nguyen, *Czech. J. of Phys.* **54**, 365 (2004).
- [11] A. Pattanaporkratana, C.S. Park, J.E. MacLennan, and N.A.Clark, *Ferroelectrics* **310**, 275 (2004).
- [12] P. Saffman, *J. Fluid Mech.* **73**, 593 (1976).
- [13] R. Holyst, A. Poniewierski, P. Fortmeier, and H. Stegemeyer, *Phys. Rev. Lett.* **81**, 5848 (1998).
- [14] Spiral brushes in smectic C islands have been reported in R. B. Meyer, D. Kononov, I. Kraus, and J. Lee, *Mol. Cryst. Liq. Cryst.* **364**, 123 (2001).
- [15] V.V. Ginzburg, R. Shao, N.A. Clark, and D.M. Walba, *Proceedings of the Society of Photo-optical Instrumentation Engineers* **2175**, 102-107 (1994).
- [16] C. Rosenblatt and N.M. Amer, *Appl. Phys. Lett.* **36**, 432 (1980).
- [17] P.G. de Gennes and J. Prost, *The Physics of Liquid Crystals* (Clarendon, Oxford, 1993).
- [18] C.Y. Young, R. Pindak, N.A. Clark, and R.B. Meyer, *Phys. Rev. Lett.* **40**, 773 (1978); C. Rosenblatt; R. Pindak, N.A. Clark, and R.B. Meyer, *Phys. Rev. Lett.* **42**, 1220 (1979); C. Rosenblatt, R.B. Meyer, R. Pindak, and N.A. Clark, *Phys. Rev. A*, **21**, 140 (1980); M.- H. Lu, K.A. Crandall, and C. Rosenblatt, *Phys. Rev. Lett.* **68**, 3575 (1992).
- [19] R.B. Meyer, L. Liebert, L. Strzelecki, and P. Keller, *J. Phys. (Paris), Lett.* **36**, L69 (1975).
- [20] Studies of films with higher polarization ($P = 40 \text{ nC/cm}^2$ in [6], and $P = 200 \text{ nC/cm}^2$ in [13]) suggest that radial alignment of the c-director (tangential \mathbf{P}) is preferred at the boundaries of inclusions and at layer steps in these materials.